# Interest of micro-reactors for the implementation of advanced electrocatalytic oxidation with boron-doped diamond anode for wastewater treatment

Emmanuel Mousset

# Interest of micro-reactors for the implementation of advanced electrocatalytic oxidation with boron-doped diamond anode for wastewater treatment

Emmanuel Mousset[1,*]

[1] Université de Lorraine, CNRS, LRGP, F-54000 Nancy, France

**ACCEPTED IN**

***Current Opinion in Electrochemistry* journal**

**(Special issue "Diamond Electrochemistry")**

* Corresponding author's email: emmanuel.mousset@cnrs.fr (Emmanuel Mousset)

# Abstract

Boron-doped diamond (BDD) anode has attracted great attention in the last two decades for its surpassing performance in advanced electro-oxidation treatment of wastewater and disinfection. Due to the heterogeneous-like oxidation of organic pollutants, more suitable electrochemical reactor designs have been more recently proposed for optimal degradation and mineralization with BDD anode. Microfluidic reactors have emerged as promising alternative, by implementing submillimetric interelectrode gap in flow-by or flow-through parallel-plate system. Micro-reactors allow intensifying the mass transport of species towards the electrode, while reducing the energy consumption and avoiding the addition of supporting electrolyte. The principle and main influencing operating parameters have been discussed in this review. Perspectives of reactive electro-mixing reactor could permit to combine micro- with macro - reactors by increasing the treatment capacity while limiting the clogging effect. Further researches are required to overcome the drawbacks of micro-reactors and to benefit from electro-precipitation phenomena for the recovery of value-added compounds.



# Keywords:

Anodic oxidation; Hydroxyl radicals; Intensification; Mass transfer; Microfluidic; Reactor design

## 1. Introduction

Boron-doped diamond (BDD) anode has been widely implemented for advanced electro-oxidation treatment of wastewater in the last two decades [1–5]. Its large potential window allows for high oxygen ($O_2$) evolution overvoltage (2.4-2.6 V vs standard hydrogen electrode (SHE)), which permit the water ($H_2O$) oxidation into physisorbed hydroxyl radical ($^{\bullet}OH$) (Eq. 1) [1,6].

$$BDD + H_2O \rightarrow BDD(^{\bullet}OH) + H^+ + e^- \quad (1)$$

This latter species is very reactive, especially with organic compounds, which make it quasi non-selective towards organic pollutants released in wastewater effluents (Eq. 2) [7,8].

$$BDD(^{\bullet}OH) + \text{compounds} \rightarrow BDD + \text{oxidation products} \quad (2)$$

Thus, BDD anode play a catalyst role in the anodic oxidation process. Moreover, $^{\bullet}OH$ has a very short lifetime ($10^{-9}$ s), which means that the reactions with $^{\bullet}OH$ take place at the vicinity of the anode, i.e. within the first tens of nanometers from BDD surface [9,10]. Therefore, the mechanism can be assimilated to a heterogeneous oxidation [11]. This means that the ratio of electrode surface per volume of solution has to be maximized. Furthermore, most of the lab-scale studies are operated with the addition of a supporting electrolyte, because the salinity of wastewater has to be minimal to run the electrolysis [12,13]. This needs to be avoided in real wastewater treatment application to avert additional pollution that will have to be removed then.

It results that the reactor design need to be adapted to favor the electrocatalytic oxidation mechanisms [14], while allowing to operate with diluted and low conductivity effluents by transfer intensification. This is in this context that microfluidic electrochemical reactors for wastewater treatment have been proposed since 2010 [15–17]. It consists of operating micrometric inter-electrode gap, which make increase the ratio of electrode surface per reactor volume. This feature is essential for a heterogeneous process such as the anodic oxidation process involved with BDD material and particularly when dealing with diluted pollution like most of the wastewaters. This review therefore aims at presenting the principle of micro-reactors implemented for wastewater treatment using BDD anode by highlighting the impact on mass transport and ohmic resistance. The main operating parameters (i.e. electrodes gap,

current density, flow rate, electrolyte conductivity, reactors configurations) influencing the microfluidic reactors have been then exposed before concluding with the main output and some promising perspectives.

## 2. Principle of micro-reactors: importance of mass transport and internal ohmic resistance considerations for BDD-based heterogenous oxidation enhancement

Three kinds of micro-reactors design have been implemented in electrochemical treatments of wastewater, the flow-by (Figs. 1a, 1b) [18–21] and flow-through (Fig. 1c) [16,22] filter-press cells as well as the reactive electro-mixing (REMix) reactor (Fig 1d) [17]. In the two first configurations, the effluent flow in between (flow-by) or through (flow-through) parallel-plate electrodes, whose distances are minimized until few tens micrometers range. In the more recent REMix system, each blade (i.e, electro-blade) of the mixer is composed of a flow-through micro-cell, in which the cathode and anode are also separated with a spacer having a thickness in micrometer range. The impeller, composed of several electro-blades, is immersed in a tank playing the role of macro-reactor.

For heterogeneous reaction, and particularly in diluted media, it is well-established that the mass transport become easily the kinetic rate-limiting step. Considering this assumption, the expression of conversion yield only depends on the mass transfer coefficient ($k_m$), the ratio of electrode surface area per volume of solution to treat and the residence time [17,23]. In addition, these parameters need to be maximized to improve the electrocatalytic reaction rate and yield. One of the key parameters to improve $k_m$, independently to the flow rate, is to optimize the reactor design. It is commonly approved that micro-reactors intensify the transfers [24–26], and it has been recently shown that $k_m$ increased non-linearly from millimetric (3 mm: $1.61\ 10^{-5}$ $ms^{-1}$) to micrometric (100 µm: $3.94\ 10^{-5}$ $ms^{-1}$) interelectrode distance ($d_{elec}$) in a flow-by parallel-plate electrochemical system and in a laminar regime using graphite cathode and BDD anode (Eq. 3 and Fig. 2a) [27]:

$$k_m = \frac{2.94\ D_L^{2/3}\ {u_L}^{1/3}\ W\ L^{2/3}}{S\ {d_{elec}}^{1/3}} \quad (3)$$

where $W$ is the electrode width (in m), $D_L$ is the diffusion coefficient (in $m^2$ $s^{-1}$), $L$ is the electrode length (in m), $S$ is the surface area (in $m^2$), $u_L$ is the cross-sectional velocity (in m $s^{-1}$).

Interestingly, a drastic increase of $k_m$ was noticed at submillimetric $d_{elec}$ (Fig. 2a), which has been identified as the limit (i.e., 1000 µm) of behavior between microfluidic and macrofluidic electrochemical systems [27]. A faster mass transfer was also announced in a study comparing micro- with macro- reactors for the abatement of tetrachloroethane in water using BDD anode [28]. The thin-film cells design therefore strongly favor the mass transport of pollutants towards the BDD material for its subsequent advanced electro-oxidation.

Furthermore, another interesting feature of micro-reactors is their ability to reduce the internal ohmic resistances, which then reduces the cell potential and therefore the energy consumption. This constitutes another advantage of the micro-reactor over the macro-reactor. For instance, for $d_{elec}$ varying from 400 to 1000 and 6000 µm, the resistance increased from 6 to 11 and 36 Ω, respectively, using mixed metal oxides anode (52.8 $cm^2$) and stainless steel cathode at 20°C of solution and 105 L $h^{-1}$ of flow rate (Fig. 2b) [16,22].

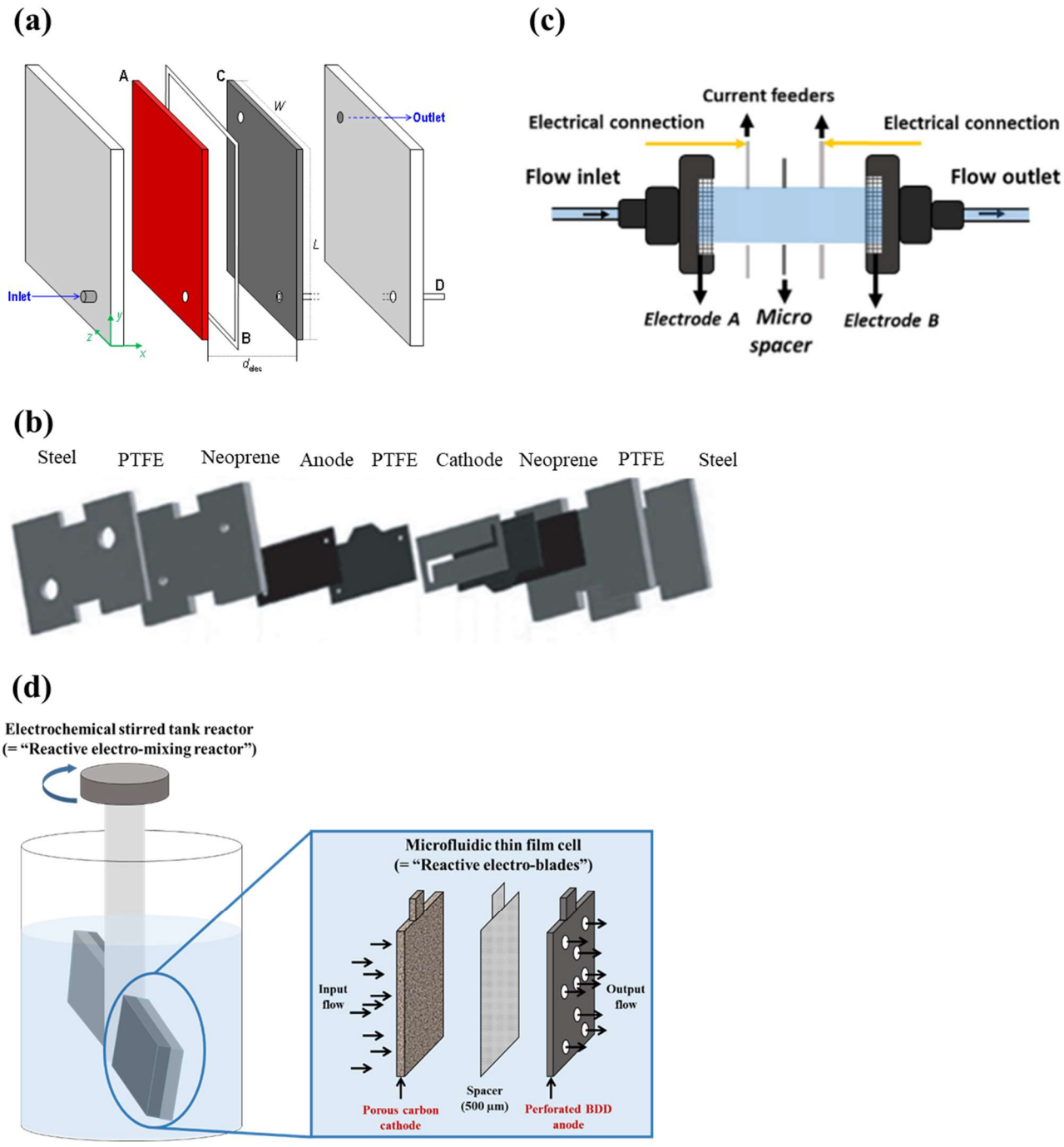


**Fig. 1.** Micro-reactor designs proposed in literature for wastewater treatment using BDD anode: (a ([27]), b ([20])) flow-by parallel-plate cells (reprinted with permission from [27] and [20]. Copyrights 2021 & 2018, Elsevier), (c) flow-through parallel-plate cell (reprinted with permission from [22]. Copyright 2018, Elsevier), (d) reactive electro-mixing reactor (reprinted with permission from [17]. Copyright 2020, Elsevier).

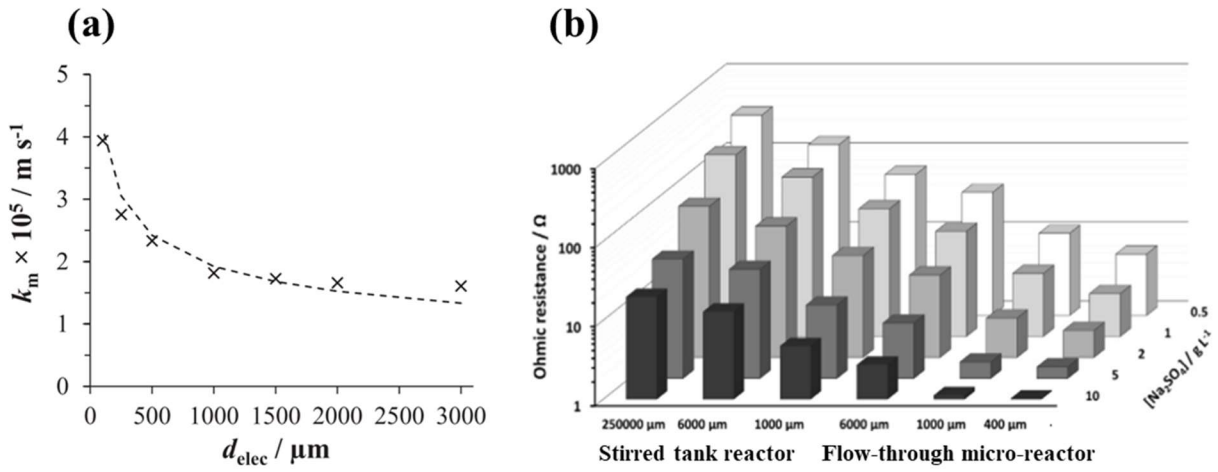


**Fig. 2.** Evolution of $k_m$ in flow-by parallel-plate cell with varying $d_{elec}$ from millimetric to submillimetric range (reprinted with permission from [27]. Copyright 2021, Elsevier) (a), evolution of ohmic resistance in flow-through micro-reactor compared to stirred tank reactor with varying $d_{elec}$ (adapted with permission from [22]. Copyright 2018, Elsevier) (b).

## 3. Influence of main operating parameters on electro-oxidation efficiency with BDD anode in micro-reactors

The main papers dealing with the implementation of BDD anode in microfluidic thin film reactors have been listed in Table 1. The influence of the main operating parameters in the wastewater treatment efficiency of electrochemical microfluidic reactors are presented in this section.

### 3.1. Influence of interelectrode gap

Though the mass transfer increase with decreasing $d_{elec}$ (Fig. 2a), it has been shown that an optimal distance is required to gain optimal degradation efficiency. An optimal distance of 500 µm has been found in the degradation of acetaminophen in flow-by micro-reactor with BDD anode (50 cm$^2$) (Fig. 3a) [29].

The existence of an optimal gap value was attributed to the occurrence of hydrogen ($H_2$) and oxygen ($O_2$) gas bubbles at both cathode (Eq. 4) and anode (Eq. 5) that could hamper the oxidation reactions at narrow gap [18,30].

$$2H_2O \rightarrow O_{2(g)} + 4H^+ + 4e^- \quad (4)$$

$2H^+ + 2e^- \rightarrow 2H_{2(g)}$ (5)

Moreover, implementing low $d_{elec}$ lead to the reduction of cell potential and therefore to the cathode and anode potentials at a given current density. However, at too low $d_{elec}$ those potentials are so low that no faradaic reactions can occur. Under this operating conditions, advanced electro-oxidation with BDD cannot be involved, due to the large overpotential required for physisorbed •OH electrogeneration. This further justify the need of an optimal $d_{elec}$.

### 3.2. Influence of current density

The current density, through electrode potential, is known to be the driving force in the removal of organic pollutant efficiency. An increase of current led to increase of •OH production rate and yield, and therefore to the increase of removal efficiency. However, there is an optimal value as often noticed in literature. An optimal current density of 4 mA $cm^{-2}$ was obtained with acetaminophen degradation in flow-by micro-reactor ($d_{elec}$: 500 µm) [29]. This corroborated the trends obtained for the abatement of 1,1,2,2-tetrachloroethane ($d_{elec}$: 50 µm) and acid orange 7 ($d_{elec}$: 50 µm), in which a current density of 12 and 10 mA $cm^{-2}$, respectively, was found optimal (Fig. 3b). Too high current densities make increase the rates of parasitic reactions such as $O_2$ (Eq. 4) and $H_2$ (Eq. 5) evolutions.

### 3.3. Influence of flow rate

It is well-established that the increase of flow rate makes increase $k_m$ [18,22]. However, the residence time is diminished in the meantime. Therefore, there is often an optimal flow rate to be applied. For instance, when the flow rate was varied from 0.1 to 0.4 mL $min^{-1}$, the degradation yield of 1,1,2,2-tetrachloroethane decreased in the meantime at the lowest applied current density (3 mA $cm^{-2}$) (Fig. 3c) [28]. In this condition, the kinetics was under current control and therefore the increase of $k_m$ did not influence the process efficiency. Contrastingly, at higher current densities (12 and 15 mA $cm^{-2}$), the kinetics were under mass transport control and the flow rate of 0.2 mL $min^{-1}$ allowed reaching the maximal abatement of the pollutant (Fig. 3c). This could be ascribed to the fact that the lower residence time in 0.2 mL $min^{-1}$ configuration was compensated by the higher mass transfer as compared to 0.1 mL $min^{-1}$ experiment. This trend was in agreement with other research [19].

Furthermore, the flow rate, and therefore the residence time, has shown to impact the formation of by-products [28]. Lower flow rates induced lower generation of chlorinated intermediates, since they had more time to be subsequently mineralized.

### 3.4. Influence of electrolyte conductivity

The increase of electrolyte conductivity is well-known to decrease the ohmic resistance (Fig 2b). It allows minimizing the rise of temperature due to high ohmic drop in the electrolyser.

The increase of conductivity from 1 to 70 mS $cm^{-1}$ (0.0035 mM to 1 M $Na_2SO_4$) has shown to decrease rapidly the ohmic resistance from around 6 Ω to around 0.6 Ω (Fig 3d) [31]. It was further noticed that the ohmic resistance of the electrolyte was preponderant in the total ohmic resistance of the flow-through microfluidic cell [31]. This further justified the need to reduce the electrolyte resistance.

Moreover, increasing the solution conductivity from 0.25 to 2 mS $cm^{-1}$ made increase the apparent rate constant of acetaminophen degradation non-linearly [29]. Knowing that real municipal wastewater effluents have an average conductivity of 1 mS $cm^{-1}$, it would suggest that the degradation would be almost optimal with the microfluidic configuration without further addition of electrolyte. Moreover, considering that most of the supporting electrolytes are sulfate- and chlorine-based media, the implementation of micro-reactors would limit the generation of hazardous chlorinated by-products (trihalomethanes, chlorate, perchlorate [32–34]) in low conductivity wastewater.

### 3.5. Influence of reactor configuration and design

The implementation of micro-reactors in series was proposed to increase the total surface area of the electrodes. The use of three micro-reactors instead of one led to an increase of total organic carbon (TOC) removal from 40% to 90% and of productivity from 2.3 to 5.3 mg-TOC $h^{-1}$, while the increase of energy was less in proportion (from 0.06 to 0.09 kWh g-$TOC^{-1}$) [35].

In other studies, flow-by configuration has been compared with the flow-through cell. The latter configuration depicted faster kinetics of degradation and mineralization as compared to flow-by cell. This has been demonstrated with clopyralid pollutant elimination for which only 2.4

Ah $L^{-1}$ was required in flow-through mode ($d_{elec}$: 400 µm) for complete mineralization, while it was required 11.4 Ah $L^{-1}$ in conventional commercial flow-by cell ($d_{elec}$: 3000 µm) [16]. Considering that the conditions (current density, electrode size, volume of effluent) were the same in both configurations, this trend could be explained by the higher mass transfer and specific surface area of electrode in flow-through compared to the flow-by modes. The $k_m$ values increased by 70% in the flow-through compared to flow-by systems (Fig. 3e) [16]. In the meantime, the energy consumption was drastically decreased in flow-through (12.5 kWh $m^{-3}$) in regards with flow-by (75.0 kWh $m^{-3}$) modes. This was due to the smaller ohmic drop with the flow-through configuration.

More recently, the efficiency of a REMix reactor has been compared with a more conventional flow-by filter press cell, in which micro-distances (500 µm) have been used in both designs [17]. The electro-oxidation with BDD anode was tested at 4 mA $cm^{-2}$ in both configurations to degrade acetaminophen as model pharmaceutical pollutant in synthetic wastewater having a low conductivity (850 µS $cm^{-1}$). At comparable residence time, the apparent rate constant of contaminant degradation was higher with the REMix design (4238 $min^{-1}$) than with the static microfluidic filter press cell (3200 $min^{-1}$). Moreover, the superiority of REMix reactor was obtained with a ratio of electrode surface per volume of solution (28/4) that was 36 times lower than with the static cell (50/0.2). The outperformance of rotating cells could be attributed to the mass transfer enhancement, while the contact between the electrode and the solution seemed increased. Furthermore, the energy requirement after 90 min of electrolysis was decreased by 20 times with the REMix configuration (0.22 kWh $m^{-3}$) compared to the static parallel-plate design (4.6 kWh $m^{-3}$). The movement of electrochemical cells could have diminished the resistance between the electrodes, so that the cell voltage could have been reduced.

It remains also essential to note that the shapes of electrodes have to be adapted to the reactor design proposed and inversely. For instance, flow-through mode imply that the electrode material should be at least perforated or be porous. For instance, a perforated BDD has been used with the REMix design [17], while a 3D mesh BDD anode has been implemented in a static microfluidic flow-through reactor [22]. This also means that the active surface area can potentially increase compared to typical planar electrode materials and can therefore play an additional role in the electro-oxidation efficiency [22,36,37].

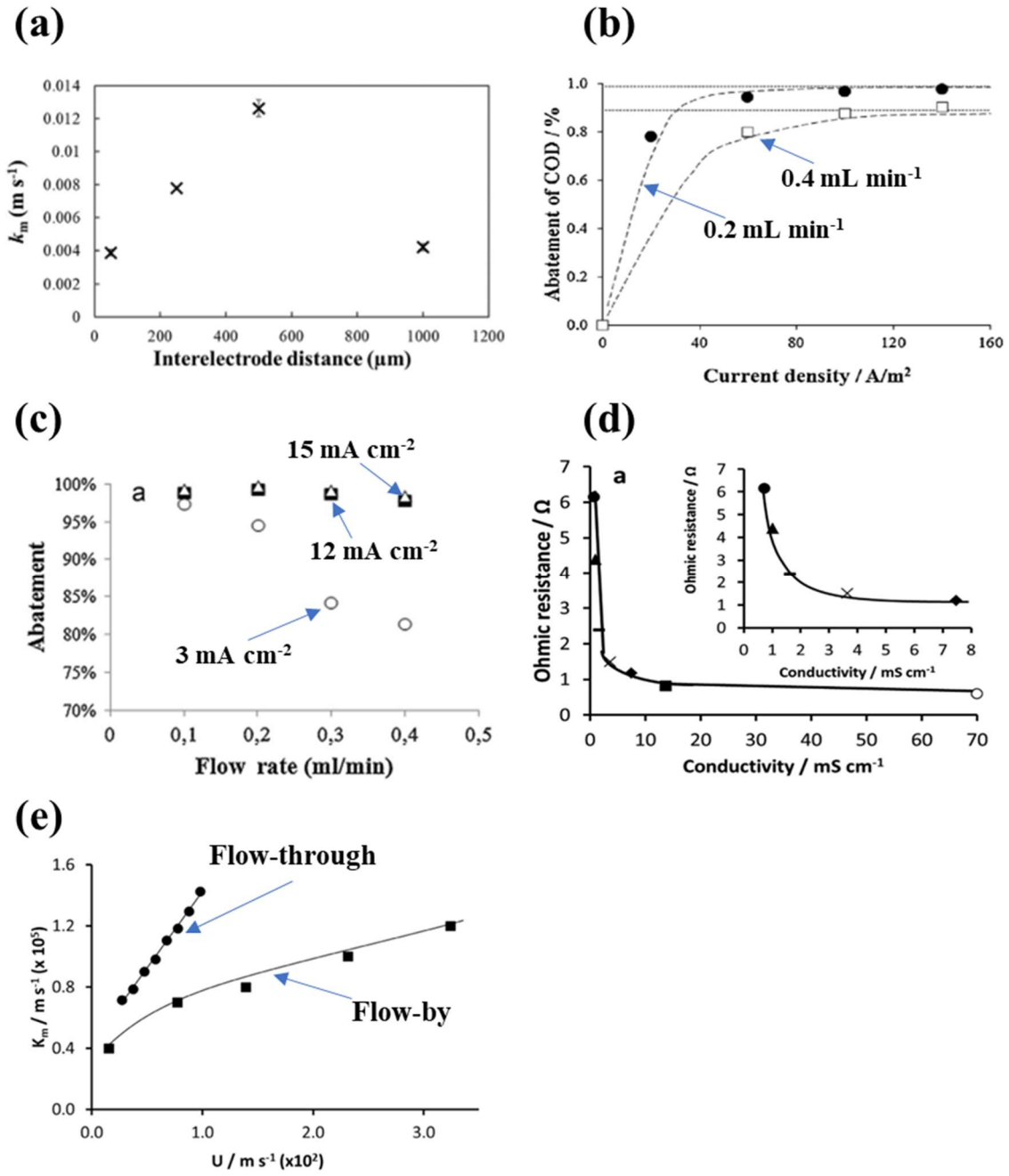


**Fig. 3.** Influence of the main parameters in micro-reactor configurations: (a) interelectrode gap (reprinted with permission from [29]. Copyright 2019, Wiley), (b) current density (adapted with permission from [38]. Copyright 2014, Elsevier), (c) flow rate (adapted with permission from [28]. Copyright 2012, Elsevier), (d) electrolyte conductivity (reprinted with permission from [31]. Copyright 2019, Elsevier), (e) reactor configuration: comparison between flow-through and flow-by cells (adapted with permission from [22]. Copyright 2018, Elsevier).

**Table 1.** Summary of reports on the implementation of BDD anode in microfluidic thin film reactors.

| Characteristics of the reactor(s) | Electrode materials | Characteristics of electrolyte | Operating conditions | Studied parameters | Efficiency | Ref. |
|---|---|---|---|---|---|---|
| - Microfluidic reactor: undivided flow-by filter-press cell; $d_{elec}$: 50-240 µm<br>- Macrofluidic reactor: undivided cylindrical stirred tank reactor; $d_{elec}$: 2 cm | - Anode: BDD-Nb, Ti/$IrO_2$–$Ta_2O_5$ or Ti/$RuO_2$–$IrO_2$ (5 $cm^2$)<br>- Cathode: Ni, graphite, carbon felt or carbon-PTFE air diffusion electrode (5 $cm^2$) | Acid orange 7 (0.43 mM) at pH 3 ($H_2SO_4$)<br><br>Supporting electrolyte: $Na_2SO_4$ (35 mM) in macroreactor | Current density: 2-14 mA $cm^{-2}$; flow rate: 0.05-0.4 mL $min^{-1}$ | $d_{elec}$, reactor design, electrode materials, current density, flow rate | 100% of COD abatement with 10 mA $cm^{-1}$ using the optimal BDD anode/graphite cathode configuration | [38] |
| Microfluidic reactor: undivided flow-by filter-press cell; $d_{elec}$: 50 and 75 µm | - Anode: BDD-Nb (2.7 $cm^2$)<br>- Cathode: Ni (2.7 $cm^2$) | Formic acid (5 mM), pH 2 ($H_2SO_4$) | Current density: 2-40 mA $cm^{-2}$; flow rate: 0.2-0.4 mL $min^{-1}$ | $d_{elec}$, current density, flow rate, inlet concentration | 100% of formic acid abatement at 10 mA $cm^{-2}$ as optimal current density | [21] |
| - Microfluidic reactor: undivided flow-by filter-press cell; $d_{elec}$: 50 µm and 100 µm<br>- Two macrofluidic reactors: undivided cylindrical stirred tank reactor; $d_{elec}$: 4 mm and 1 cm | - Anode: BDD-Nb or Ti/$IrO_2$–$Ta_2O_5$ (3, 5, 10 $cm^2$)<br>- Cathode: graphite or | Monochloroacetic acid (5 mM), pH 3 ($H_2SO_4$) | Current density: 2-20 mA $cm^{-2}$; flow rate: 0.05-0.6 mL $min^{-1}$ (micro-reactor) and 1 L $min^{-1}$ (macroreactor) | $d_{elec}$, reactor design, electrode materials, current density, flow rate | 100% abatement with graphite cathode and BDD anode and 5 mA $cm^{-2}$ | [39] |

| | | | | | | |
|---|---|---|---|---|---|---|
| | stainless steel (3, 5, 10 $cm^2$) | | | | | |
| Microfluidic reactor: undivided flow-by filter-press cell; $d_{elec}$: 50 µm and 75 µm | - Anode: BDD-Nb or DSA (3-4 $cm^2$)<br>- Cathode: Ni or Ag (3-4 $cm^2$) | 1,1,2,2-tetrachloroethane (0.9 mM), pH 2 ($H_2SO_4$) | Current density: 2-40 mA $cm^{-2}$; flow rate: 0.1-0.4 mL $min^{-1}$ | $d_{elec}$, electrode materials, current density, flow rate | Better efficiencies at lower distances | [28] |
| Microfluidic reactor: undivided flow-by filter-press cell; $d_{elec}$: 50 µm and 120 µm | - Anode: BDD-Nb or Ti/$IrO_2$–$Ta_2O_5$ (3-4 $cm^2$)<br>- Cathode: Ni or Ag (3-4 $cm^2$) | Acid orange 7 (150-500 mg $L^{-1}$) at pH 3 ($H_2SO_4$) | Current density: 2-20 mA $cm^{-2}$; flow rate: 0.1-0.3 mL $min^{-1}$ | $d_{elec}$, electrode materials, current density, flow rate | Highest TOC removal (89%) with configuration of 2, 2 and 20 mA $cm^{-2}$ (0.9 kWh g-$TOC^{-1}$) | [35] |
| Microfluidic reactor: undivided flow-by filter-press cell; $d_{elec}$: 50 µm<br><br>Macrofluidic reactor: undivided cylindrical stirred tank reactor; $d_{elec}$: 2 cm | - Anode: BDD-Nb (3.75 $cm^2$)<br>- Cathode: Ni (3.75 $cm^2$) | Real industrial wastewater (conductivity: 1.4 mS $cm^{-1}$, pH 6.2, TOC = 210 mg-C $L^{-1}$) | Current intensity: 20-200 mA $cm^{-2}$; electrolyte concentration: $Na_2SO_4$ (0.03-0.2 M) and $NaClO_4$ (0.1-0.2 M); flow rate: 0.1-0.5 mL $min^{-1}$ | Current density, electrolyte concentration, flow rate | 79% (micro-reactor) against 70% (macro-reactor) in TOC removal at 100 mA without supporting electrolyte, corresponding to 1.0 and 19.8 € $m^{-3}$ of electric energy cost, respectively | [20] |

| | | | | | | |
|---|---|---|---|---|---|---|
| Microfluidic reactor: undivided flow-through filter-press cell; $d_{elec}$: 400 µm<br><br>Macrofluidic reactor: undivided flow-by filter-press cell; $d_{elec}$: 3 cm | - Anode: 3D-mesh BDD-Nb (33 $cm^2$) (BDD: 78 $cm^2$ in macro-reactor)<br>- Cathode: perforated stainless steel (33 $cm^2$) | Clopyralid (100 mg $L^{-1}$) in synthetic brackish natural water (conductivity: 1 mS $cm^{-1}$, $Cl^-$: 79.9, $NO_3^-$: 94.9, $SO_4^{2-}$: 259.8 mg $L^{-1}$, $CO_3^{2-}$ = 174.8, $Ca^{2+}$: 116.5) | Current density: 10 mA $cm^{-2}$, flow rate: 1.7 (flow-through) and 0.8 (flow-by) L $min^{-1}$ | Reactor design | Flow-through: 2.3 Ah $L^{-1}$ for total mineralization (12.5 kWh $m^{-3}$)<br><br>Flow-by: 11.4 Ah $L^{-1}$ for total mineralization (75 kWh $m^{-3}$) | [16] |
| Microfluidic reactor: undivided flow-through filter-press cell; $d_{elec}$: 400, 1000, 6000 µm<br><br>Macrofluidic reactor: undivided flow-by filter-press cell; $d_{elec}$: 3 cm | - Anode: 3D-mesh BDD-Nb (33 $cm^2$) (BDD: 78 $cm^2$ in macro-reactor)<br>- Cathode: perforated stainless steel (33 $cm^2$) | Clopyralid (100 mg $L^{-1}$) in synthetic brackish natural water (conductivity: 1 mS $cm^{-1}$) | Current density: 10 and 100 mA $cm^{-2}$; flow rate: 1.7 (flow-through) and 0.8 (flow-by) L $min^{-1}$ | $d_{elec}$, current density | The microfluidic flow-through required from 4 to 10 times less electric charge and from 6 to 15 times less energy for the mineralization | [22] |
| Microfluidic reactor: undivided flow-through filter-press cell; $d_{elec}$: 400, 1000, 6000 µm | - Anode: 3D-mesh BDD-Nb or $RuO_2/IrO_2$ (33 $cm^2$)<br>- Cathode: carbon black/PTFE-reticulated vitreous | Clopyralid (100 mg $L^{-1}$) at pH 3 ($H_2SO_4$), 0.5 mM iron and 7 mM $Na_2SO_4$ | Current density: 20 mA $cm^{-2}$; flow rate: 1.2 L $min^{-1}$ | Electrode materials, electrolyte concentration | Complete degradation after 0.44 Ah $L^{-1}$ and 0.02 kWh $g^{-1}$ with the optimal BDD anode and carbon black/PTFE-aluminum configuration | [40] |

| | | | | | | |
|---|---|---|---|---|---|---|
| | carbon, carbon black/PTFE-aluminum, perforated stainless steel (33 $cm^2$) | | | | | |
| Microfluidic reactor: undivided flow-through filter-press cell; $d_{elec}$: 150 µm | - Anode: 3D-mesh BDD-Nb (33 $cm^2$)<br>- Cathode: carbon black/PTFE-aluminum or perforated stainless steel (33 $cm^2$) | Clopyralid (20-30 mg $L^{-1}$) at pH 3 ($H_2SO_4$), 0.5 mM iron | Current density: 10-100 mA $cm^{-2}$; flow rate: 0.4, 1.0, 1.6 L $min^{-1}$ | Electrode materials, flow rate | Faster removal (100%) at 10 mA $cm^{-2}$ | [41] |
| Microfluidic reactor: undivided flow-by filter-press cell; $d_{elec}$: 50, 250, 500, 1000 µm | - Anode: BDD-Nb (50 $cm^2$)<br>- Cathode: carbon felt (50 $cm^2$) | Acetaminophen (0.1 mM) in synthetic and reclaimed municipal wastewater (conductivity: 0.86 mS $cm^{-1}$) | Current density: 2-12 mA $cm^{-2}$; flow rate: 0.43 L $min^{-1}$; electrolyte concentration: $Na_2SO_4$ (1-10 mM) | $d_{elec}$, current density, electrolyte concentration | 0.18 $kWhg^{-1}$ for an 84% of acetaminophen degradation | [29] |
| Microfluidic reactor: undivided flow-by filter-press cell; $d_{elec}$: 500 µm | - Anode: BDD-Nb or Pt (50 $cm^2$) | Simulated reclaimed municipal wastewater containing calcium (150 mg $L^{-1}$), magnesium (5 mg $L^{-}$ | Current density: 0.4 and 4 mA $cm^{-2}$ | Current density | Electro-precipitation of $Mg(OH)_2$ and $CaCO_3$ | [18] |

| | | | | | | |
|---|---|---|---|---|---|---|
| | - Cathode: stainless steel (50 $cm^2$) | $^{1}$), carbonate (60 mg-C $L^{-1}$), $Na_2SO_4$ (5 mM) | | | | |
| Two microfluidic reactors (reactive electro-blades) in rotation in a macro-reactor (REMix reactor): undivided flow-through filter-press cells; $d_{elec}$: 500 µm<br><br>Microfluidic reactor: undivided flow-by filter-press cell; $d_{elec}$: 500 µm | - Anodes: perforated BDD-Nb (14 $cm^2$ each; 50 $cm^2$ in flow-by static micro-reactor)<br>- Cathodes: carbon felt (14 $cm^2$ each in REMix reactor; 50 $cm^2$ in flow-by static micro-reactor) | Acetaminophen (0.1 mM) in synthetic municipal wastewater (conductivity: 0.86 mS $cm^{-1}$, $Na_2SO_4$ (4 mM)) | Current intensity: 2*200 mA (REMix reactor); current density: 4 mA $cm^{-2}$ and flow rate: 0.43 L $min^{-1}$ (flow-by cell) | Reactor design | Apparent decay rate constant of 4,238 $min^{-1}$ with REMix reactor compared to 3,200 $min^{-1}$ with conventional static flow-by microfluidic reactor | [17] |

## 4. Concluding remarks and future perspectives

Through this literature review, it can be mainly highlighted the fact that it is not at the lowest electrode distance and flow rate as well as at the highest current density and solution conductivity that the removal efficiency is the best. There are existences of optimal value of these main operating parameters in microfluidic thin film reactors applied for wastewater treatment. It is further important in future studies to pay attention to the suitability of comparison when those parameters are varied. For instance, when the influence of $d_{elec}$ is studied it is important to perform the experiments at equivalent residence time and hydrodynamic regime by adjusting the flow rate for each $d_{elec}$ in order to be comparable. Moreover, it would be reliable to compare the efficiency between flow-through and flow-by modes at equivalent surface area of electrode, to better figure out the real effect of mass transfer. Furthermore, it is also important to note that the electric current distribution could not be homogeneous in porous materials such as those employed in flow-through configuration [42–44], unlike the planar parallel-plates used in flow-by device. This should be assessed in order to optimize the porous material properties (e.g., thickness, pore size distribution), while the implementation of BDD foam [45] with preliminary valid long-term stability tests could be examined with micro-reactors.

It has been also emphasized that micro-reactors provide undoubtedly advantages – especially in flow-through compared to flow-by configurations - such as the increase of kinetics of degradation/mineralization efficiency, the absence of supporting electrolyte addition in low-conductivity effluents as well as the strong energy consumption reduction. However, there are challenges to overcome such as the clogging effects with real wastewater and the low treatment capacity due to the very narrow gap between electrodes. A recent study introduced the concept of “reactive electro-mixing” that allows mixing while operating multiple electro-processes simultaneously within the same scalable reactor, combining micro- with macro-reactors and operating with liquid and semi-liquid effluents [17]. The advantages of micro-reactors (transfer intensification, ohmic drop reduction) could be therefore combined with macro-reactors (high treatment capacity, less clogging issue) along with synergies by operating them in a hybrid system. Still, this latter system needs to be characterized in the aim at better understanding the roles of hydrodynamics and cell rotation on the reactions efficiency. Moreover, the impact of fouling has to be tested in order to know whether a pre-filtration step would be required or not before the electro-oxidation of wastewater with BDD, as it would be commonly considered with static micro-reactors.

Moreover, there could be scaling issues in the electrolyzer, especially when dealing with real wastewater effluents [46,47]. Mineral scaling in electrochemical reactors is a well-known phenomenon that induces most of the time the passivation of the cathode and therefore hamper the electrolysis [48,49]. This is due mainly to the ubiquitous presence of calcium, magnesium and/or carbonates in the effluents to treat [18]. Thus, the local alkalization that occurs at the cathode lead to their electro-precipitation [50–52]. An early recent study has shown that the microfluidic thin film ($d_{elec}$: 500 µm) reactor configuration did not limit the electro-precipitation of $Mg(OH)_2$ and $CaCO_3$ [18]. The local acidification at anode did not compensate enough the alkalization at cathode in the parallel-plate micro-reactor. Thus, further researches are required to surpass the micro-reactors drawbacks. Moreover, some electro-precipitation issues could be turned into advantages by recovering added-value compounds such as phosphate [53], while studying more deeply the influence of $d_{elec}$ and electrode/electrolyte interface phenomenon.

## Acknowledgments

The author gratefully acknowledges the support by the French National Research Agency (ANR) through the REMixSyn project (n°ANR-21-CE04-0006-01).

## References and recommended reading

[1] C.A. Martínez-Huitle, M. Panizza, Electrochemical oxidation of organic pollutants for wastewater treatment, Curr. Opin. Electrochem. 11 (2018) 62–71. https://doi.org/10.1016/j.coelec.2018.07.010.

[2] S.O. Ganiyu, C.A. Martínez-Huitle, The use of renewable energies driving electrochemical technologies for environmental applications, Curr. Opin. Electrochem. 22 (2020) 211–220. https://doi.org/10.1016/j.coelec.2020.07.007.

[3] S. Garcia-Segura, A.B. Nienhauser, A.S. Fajardo, R. Bansal, C.L. Conrad, J.D. Fortner, M. Marcos-Hernández, T. Rogers, D. Villagran, M.S. Wong, P. Westerhoff, Disparities between experimental and environmental conditions: Research steps toward making electrochemical water treatment a reality, Curr. Opin. Electrochem. 22 (2020) 9–16. https://doi.org/10.1016/j.coelec.2020.03.001.

[4] E. Mousset, C. Trellu, H. Olvera-Vargas, Y. Pechaud, F. Fourcade, M.A. Oturan, Electrochemical technologies coupled with biological treatments, Curr. Opin. Electrochem. 26 (2021) 100668. https://doi.org/10.1016/j.coelec.2020.100668.

[5] C. Trellu, H. Olvera Vargas, E. Mousset, N. Oturan, M.A. Oturan, Electrochemical technologies for the treatment of pesticides, Curr. Opin. Electrochem. 26 (2021) 100677. https://doi.org/10.1016/j.coelec.2020.100677.

[6] E. Mousset, D.D. Dionysiou, Photoelectrochemical reactors for treatment of water and wastewater: a review, Environ. Chem. Lett. 18 (2020) 1301–1318. https://doi.org/10.1007/s10311-020-01014-9.

[7] E. Mousset, N. Oturan, M.A. Oturan, An unprecedented route of OH radical reactivity evidenced by an electrocatalytical process: Ipso-substitution with perhalogenocarbon compounds, Appl. Catal. B Environ. 226 (2018) 135–146. https://doi.org/10.1016/j.apcatb.2017.12.028.

[8] M. Panizza, G. Cerisola, Direct and mediated anodic oxidation of organic pollutants, Chem. Rev. 109 (2009) 6541–6569. https://doi.org/10.1021/cr9001319.

[9] M.A. Oturan, Outstanding performances of the BDD film anode in electro-Fenton process: Applications and comparative performance, Curr. Opin. Solid State Mater. Sci. 25 (2021) 100925. https://doi.org/10.1016/j.cossms.2021.100925.

[10] P.-A. Michaud, Comportement anodique du diamant synthétique dopé au bore, Ecole Polytechnique Fédérale de Lausanne, 2002.

[11] E. Mousset, Y. Pechaud, N. Oturan, M.A. Oturan, Charge transfer/mass transport competition in advanced hybrid electrocatalytic wastewater treatment: Development of a new current efficiency relation, Appl. Catal. B Environ. 240 (2019). https://doi.org/10.1016/j.apcatb.2018.08.055.

[12] S. Garcia-Segura, J.D. Ocon, M.N. Chong, Electrochemical oxidation remediation of real wastewater effluents — A review, Process Saf. Environ. Prot. 113 (2018) 48–67. https://doi.org/10.1016/j.psep.2017.09.014.

[13] O. Garcia-Rodriguez, E. Mousset, H. Olvera-Vargas, O. Lefebvre, Electrochemical treatment of highly concentrated wastewater: A review of experimental and modeling approaches from lab- to full-scale, Crit. Rev. Environ. Sci. Technol. 0 (2020) 1–70. https://doi.org/10.1080/10643389.2020.1820428.

[14] O.M. Cornejo, M.F. Murrieta, L.F. Castañeda, J.L. Nava, Electrochemical reactors equipped with BDD electrodes: Geometrical aspects and applications in water treatment, Curr. Opin. Solid State Mater. Sci. 25 (2021). https://doi.org/10.1016/j.cossms.2021.100935.

**[15]O. Scialdone, C. Guarisco, A. Galia, G. Filardo, G. Silvestri, C. Amatore, C. Sella, L. Thouin, Anodic abatement of organic pollutants in water in micro reactors, J. Electroanal. Chem. 638 (2010) 293–296. https://doi.org/10.1016/j.jelechem.2009.10.031.

→First paper implementing micro-reactors for wastewater treatment application.

**[16]J.F. Pérez, J. Llanos, C. Sáez, C. López, P. Cañizares, M.A. Rodrigo, A microfluidic flow-through electrochemical reactor for wastewater treatment: A proof-of-concept,

Electrochem. Commun. 82 (2017) 85–88. https://doi.org/10.1016/j.elecom.2017.07.026.

→This paper presents for the first time flow-through micro-reactor configuration for wastewater treatment.

**[17]E. Mousset, Unprecedented reactive electro-mixing reactor: Towards synergy between micro- and macro-reactors?, Electrochem. Commun. 118 (2020) 106787. https://doi.org/10.1016/j.elecom.2020.106787.

→Paper that introduce for the first time the concept of "reactive electro-mixing" by combining the advantages of micro-cells with those of macro-reactor, while allowing to operate with liquid and semi-liquid media.

*[18] F.H. Adnan, E. Mousset, S. Pontvianne, M.N. Pons, Mineral cathodic electro-precipitation and its kinetic modelling in thin-film microfluidic reactor during advanced electro-oxidation process, Electrochim. Acta. 387 (2021) 138487. https://doi.org/10.1016/j.electacta.2021.138487.

→First paper proposing a predictive model of electro-precipitation of $Mg(OH)_2$ and $CaCO_3$. This is also the first time that electro-precipitation is studied in a micro-reactor under advanced electro-oxidation condition.

[19] O. Scialdone, A. Galia, S. Sabatino, G.M. Vaiana, D. Agro, A. Busacca, C. Amatore, Electrochemical conversion of dichloroacetic acid to chloroacetic acid in conventional cell and in two microfluidic reactors, ChemElectroChem. 1 (2014) 116–124. https://doi.org/10.1002/celc.201300216.

*[20] P. Ma, H. Ma, S. Sabatino, A. Galia, O. Scialdone, Electrochemical treatment of real wastewater. Part 1: Effluents with low conductivity, Chem. Eng. J. 336 (2018) 133–140. https://doi.org/10.1016/j.cej.2017.11.046.

→This is the first time that a paper deal with micro-reactors applied for real wastewater effluent treatment, and particularly with low-conductivity solution.

[21] O. Scialdone, C. Guarisco, A. Galia, Oxidation of organics in water in microfluidic electrochemical reactors: Theoretical model and experiments, Electrochim. Acta. 58 (2011) 463–473. https://doi.org/10.1016/j.electacta.2011.09.073.

[22] J.F. Pérez, J. Llanos, C. Sáez, C. López, P. Cañizares, M.A. Rodrigo, Development of

an innovative approach for low-impact wastewater treatment: A microfluidic flow-through electrochemical reactor, Chem. Eng. J. 351 (2018) 766–772. https://doi.org/10.1016/j.cej.2018.06.150.

[23] F. Coeuret, A. Storck, Eléments de génie électrochimique, 1st Ed., Tec & Doc, Paris (France), 1984.

[24] H.S. White, K. McKelvey, Redox cycling in nanogap electrochemical cells, Curr. Opin. Electrochem. 7 (2018) 48–53. https://doi.org/10.1016/j.coelec.2017.10.021.

[25] D. Russo, Kinetic modeling of advanced oxidation processes using microreactors: Challenges and opportunities for scale-up, Appl. Sci. 11 (2021) 1–19. https://doi.org/10.3390/app11031042.

[26] S. Fransen, J. Fransaer, S. Kuhn, Current and concentration distributions in electrochemical microreactors: Numerical calculations and asymptotic approximations for self-supported paired synthesis, Electrochim. Acta. 292 (2018) 914–934. https://doi.org/10.1016/j.electacta.2018.08.082.

**[27]F.H. Adnan, M.-N. Pons, E. Mousset, Mass transport evolution in microfluidic thin film electrochemical reactors: New correlations from millimetric to submillimetric interelectrode distances, Electrochem. Commun. 130 (2021) 107097. https://doi.org/10.1016/j.elecom.2021.107097.

→This research paper permit to evidence the frontier between microfluidic and macrofluidic in flow-by system, while a new correlation permit to predict the evolution of mass transfer coefficient from macro-reactor to micro-reactor configurations.

[28] O. Scialdone, A. Galia, C. Guarisco, S. La Mantia, Abatement of 1,1,2,2-tetrachloroethane in water by reduction at silver cathode and oxidation at boron doped diamond anode in micro reactors, Chem. Eng. J. 189–190 (2012) 229–236. https://doi.org/10.1016/j.cej.2012.02.062.

[29] E. Mousset, M. Puce, M.N. Pons, Advanced electro-oxidation with boron-doped diamond for acetaminophen removal from real wastewater in a microfluidic reactor: Kinetics and mass-transfer studies, ChemElectroChem. 6 (2019) 2908–2916. https://doi.org/10.1002/celc.201900182.

[30] Y. Cao, C. Soares, N. Padoin, T. Noël, Gas bubbles have controversial effects on Taylor flow electrochemistry, Chem. Eng. J. 406 (2021) 126811. https://doi.org/10.1016/j.cej.2020.126811.

[31] J.F. Pérez, J. Llanos, C. Sáez, C. López, P. Cañizares, M.A. Rodrigo, Towards the scale up of a pressurized-jet microfluidic flow-through reactor for cost-effective electro-generation of H2O2, J. Clean. Prod. 211 (2019) 1259–1267. https://doi.org/10.1016/j.jclepro.2018.11.225.

[32] E. Mousset, L. Quackenbush, C. Schondek, A. Gerardin-Vergne, S. Pontvianne, S. Kmiotek, M.N. Pons, Effect of homogeneous Fenton combined with electron transfer on the fate of inorganic chlorinated species in synthetic and reclaimed municipal wastewater, Electrochim. Acta. 334 (2020) 135608. https://doi.org/10.1016/j.electacta.2019.135608.

[33] Y. Lan, C. Coetsier, C. Causserand, K. Groenen Serrano, On the role of salts for the treatment of wastewaters containing pharmaceuticals by electrochemical oxidation using a boron doped diamond anode, Electrochim. Acta. 231 (2017) 309–318. https://doi.org/10.1016/j.electacta.2017.01.160.

[34] M.E.H. Bergmann, A.S. Koparal, T. Iourtchouk, Electrochemical advanced oxidation processes, formation of halogenate and perhalogenate species: A critical review, Crit. Rev. Environ. Sci. Technol. 44 (2014) 348–390. https://doi.org/10.1080/10643389.2012.718948.

[35] S. Sabatino, A. Galia, O. Scialdone, Electrochemical abatement of organic pollutants in continuous-reaction systems through the assembly of microfluidic cells in series, ChemElectroChem. 3 (2016) 83–90. https://doi.org/10.1002/celc.201500409.

[36] O.M. Cornejo, M.F. Murrieta, L.F. Castañeda, J.L. Nava, Characterization of the reaction environment in flow reactors fitted with BDD electrodes for use in electrochemical advanced oxidation processes: A critical review, Electrochim. Acta. 331 (2020). https://doi.org/10.1016/j.electacta.2019.135373.

[37] L.F. Arenas, C. Ponce de León, F.C. Walsh, 3D-printed porous electrodes for advanced electrochemical flow reactors: A Ni/stainless steel electrode and its mass transport characteristics, Electrochem. Commun. 77 (2017) 133–137.

435 https://doi.org/10.1016/j.elecom.2017.03.009.

436 [38] O. Scialdone, A. Galia, S. Sabatino, Abatement of acid orange 7 in macro and micro
437 reactors. Effect of the electrocatalytic route, Appl. Catal. B Environ. 148–149 (2014)
438 473–483. https://doi.org/10.1016/j.apcatb.2013.11.005.

439 [39] O. Scialdone, E. Corrado, A. Galia, I. Sirés, Electrochemical processes in macro and
440 microfluidic cells for the abatement of chloroacetic acid from water, Electrochim. Acta.
441 132 (2014) 15–24. https://doi.org/10.1016/j.electacta.2014.03.127.

442 *[40] J.F. Pérez, J. Llanos, C. Sáez, C. López, P. Cañizares, M.A. Rodrigo, On the design of a
443 jet-aerated microfluidic flow-through reactor for wastewater treatment by electro-
444 Fenton, Sep. Purif. Technol. 208 (2019) 123–129.
445 https://doi.org/10.1016/j.seppur.2018.04.021.

446 →This paper newly presents the combination of flow-through micro-reactor with jet-aerated
447 systems, which allow avoiding the addition of supporting electrolyte and $O_2$ external
448 supplier for electrochemical advanced oxidation processes.

449 [41] M. Rodríguez, M. Muñoz-Morales, J.F. Perez, C. Saez, P. Cañizares, C.E. Barrera-Díaz,
450 M.A. Rodrigo, Toward the Development of Efficient Electro-Fenton Reactors for Soil
451 Washing Wastes through Microfluidic Cells, Ind. Eng. Chem. Res. 57 (2018) 10709–
452 10717. https://doi.org/10.1021/acs.iecr.8b02215.

453 [42] J.S. Newman, C.W. Tobias, Theoretical Analysis of Current Distribution in Porous
454 Electrodes, J. Electrochem. Soc. 109 (1962) 1183. https://doi.org/10.1149/1.2425269.

455 [43] F. Coeuret, Ingénierie des procédés électrochimiques, Ellipses, Paris (France), 2003.

456 [44] A. Lissaneddine, M.-N. Pons, F. Aziz, N. Ouazzani, L. Mandi, E. Mousset, A critical
457 review on the electrosorption of organic compounds in aqueous effluent – Influencing
458 factors and engineering considerations, Environ. Res. 204 (2022) 112128.

459 [45] D. Miao, Z. Li, Y. Chen, G. Liu, Z. Deng, Y. Yu, S. Li, K. Zhou, L. Ma, Q. Wei,
460 Preparation of macro-porous 3D boron-doped diamond electrode with surface micro
461 structure regulation to enhance electrochemical degradation performance, Chem. Eng. J.
462 429 (2022). https://doi.org/10.1016/j.cej.2021.132366.

463 [46] C. Barchiche, C. Deslouis, O. Gil, P. Refait, B. Tribollet, Characterisation of calcareous

deposits by electrochemical methods: Role of sulphates, calcium concentration and temperature, Electrochim. Acta. 49 (2004) 2833–2839. https://doi.org/10.1016/j.electacta.2004.01.067.

[47] C. Deslouis, C. Gabrielli, M. Keddam, A. Khalil, R. Rosset, B. Tribollet, M. Zidoune, Impedance techniques at partially blocked electrodes by scale deposition, Electrochim. Acta. 42 (1997) 1219–1233. https://doi.org/10.1016/S0013-4686(96)00290-3.

[48] Z. Belarbi, B. Sotta, L. Makhloufi, B. Tribollet, J. Gamby, Modelling of delay effect of calcium carbonate deposition kinetics on rotating disk electrode in the presence of green inhibitor, Electrochim. Acta. 189 (2016) 118–127. https://doi.org/10.1016/j.electacta.2015.12.089.

[49] S.M. Hoseinieh, T. Shahrabi, B. Ramezanzadeh, M.F. Rad, The Role of Porosity and Surface Morphology of Calcium Carbonate Deposits on the Corrosion Behavior of Unprotected API 5L X52 Rotating Disk Electrodes in Artificial Seawater, J. Electrochem. Soc. 163 (2016) C515–C529. https://doi.org/10.1149/2.0191609jes.

[50] C. Deslouis, I. Frateur, G. Maurin, B. Tribollet, Interfacial pH measurement during the reduction of dissolved oxygen in a submerged impinging jet cell, J. Appl. Electrochem. 27 (1997) 482–492. https://doi.org/10.1023/A:1018430224622.

[51] H. Deligianni, L.T. Romankiw, In situ surface pH measurement during electrolysis using a rotating pH electrode, IBM J. Res. Dev. 37 (1993) 85–94. https://doi.org/10.1147/rd.372.0085.

[52] C. Carré, A. Zanibellato, M. Jeannin, R. Sabot, P. Gunkel-Grillon, A. Serres, Electrochemical calcareous deposition in seawater. A review, Environ. Chem. Lett. 18 (2020) 1193–1208. https://doi.org/10.1007/s10311-020-01002-z.

[53] Y. Lei, J.C. Remmers, M. Saakes, R.D. Van Der Weijden, C.J.N. Buisman, Influence of Cell Configuration and Long-Term Operation on Electrochemical Phosphorus Recovery from Domestic Wastewater, ACS Sustain. Chem. Eng. 7 (2019) 7362–7368. https://doi.org/10.1021/acssuschemeng.9b00563.